

# The Substellar Transition Zone: A Stretched Temperature Canyon in Brown Dwarf Population due to Unsteady Hydrogen Fusion

ZengHua Zhang

GEPI, Observatoire de Paris, PSL Université, CNRS, 5 Place Jules Janssen, 92190 Meudon, France

## Abstract

I introduce an L subdwarf classification scheme, which classified L subdwarfs into three metal subclasses. I would also like to draw your attention to transitional brown dwarfs which have unsteady hydrogen fusion in their cores to replenish the dissipation of their initial thermal energy. The temperature distribution of transitional brown dwarfs are stretched to a wide range and formed a substellar transition zone. The transition zone is most significant in the old halo population and range from 1000 K to 2200-3000 K depending on metallicity. The transition zone have impacts on our observational properties of field brown dwarf population. Because field L dwarfs are composed of very low-mass stars, transition brown dwarfs, and relative younger electric-degenerate brown dwarfs.

## 1 Introduction

Brown dwarfs (BDs) are substellar objects that were predicted in the 1960s (Kumar, 1963; Hayashi & Nakano, 1963) and discovered in the 1990s (Rebolo *et al.*, 1995; Nakajima *et al.*, 1995). They are the low-mass end of the initial mass function (IMF), and are very sensitive for IMF measurement. BDs overlap with exoplanets in terms of mass ( $\sim 3-90 M_J$ ) and  $T_{\text{eff}}$  ( $\sim 250-2800$  K), and are key to understand ultra-cool atmospheres and characterize of exoplanets.

However, the characterization of BD population remains a big challenge. Some spectral features of BDs are not well reproduced by the latest atmospheric models Allard (2014). The mass of stellar/substellar boundary measured by different approaches have notable differences. Firstly because BDs are faint and have ultra-cool atmospheres and complex clouds. Secondly, BDs have mass/age degeneracy; thus luminosity/ $T_{\text{eff}}$  are age dependent. It is difficult to characterize a BD without knowing its mass or age. Thirdly, the ‘substellar transition zone’ between very low-mass stars (VLMS) and electron-degenerate BDs (D-BDs) was not considered previously in the characterization of brown dwarfs.

In this paper I summarize those results on L subdwarfs, transitional BDs (T-BDs), and the substellar transition zone from a series titled *Primeval very low-mass stars and brown dwarfs* (Zhang *et al.*, 2017b,a, 2018b,a)<sup>1</sup>.

## 2 Classification of L subdwarfs

L subdwarfs have rather diverse spectral features because they are distributed into a wide range of metallicity (and opacity), and have cloud formation in their atmospheres. For example, fig. 1 shows that L subdwarfs have much bluer optical and near-infrared (NIR) colours than L dwarfs.

A three-dimension classification concept for for ultracool

dwarfs/subdwarfs was proposed by Kirkpatrick (2005). The core part of spectral types is spectral class and subtype which indicating  $T_{\text{eff}}$  and clouds. The prefix and suffix of spectral types are subclasses corresponding to different metallicity (e.g. d, sd, esd) and gravity (e.g.  $\alpha, \beta, \gamma$ ), respectively. The metal subclass is more relevant to old ultracool subdwarfs which cover a wide range of metallicity and have similar gravity. The gravity subclass is more relevant to young ultracool dwarfs which cover a wider range of gravity but a smaller range of metallicity.

The classification of L subdwarfs is mainly on their subtypes and metal subclasses. Subtypes of L subdwarfs are determined by comparing their red optical spectra to those of L dwarfs (Burgasser *et al.*, 2007; Kirkpatrick *et al.*, 2010). Zhang *et al.* (2017b) classified L subdwarfs into ultra subdwarf (usdL), extreme subdwarf (esdL), and subdwarf (sdL) subclasses, corresponding to metallicity ranges of  $[\text{Fe}/\text{H}] < -1.7$  (usdL);  $-1.7 < [\text{Fe}/\text{H}] < -1$  (esdL);  $-1 < [\text{Fe}/\text{H}] < -0.3$  (sdL). Spectral features of each subclass are summarized in table 3 of Zhang *et al.* (2017b). Fig. 1 shows that L subdwarfs of difference subclass are well separated by their optical to NIR colours.

Fig. 2 shows optical to NIR spectra of usdL4, esdL4, sdL4, dL4, and red dL4 subclasses normalized in the optical. We can see that objects with lower metallicity have bluer spectra and larger suppression in the NIR. Note that the true relative flux between spectra of different subclass are contrary as shown in Fig. 2. Fig. 22 in Zhang *et al.* (2018a) shows that L4 type spectra of different subclass have a similar  $H$ -band absolute magnitude. Therefore, a set of these L4 type spectra of different metal subclass normalized at  $H$ -band would show their true relative flux at a same distance (e.g. fig. 15 of Zhang *et al.*, 2017b). Although all classified as L4 type, the usdL4 have the highest flux at wavelengths below 1600 nm.

The spectral subtypes of L subdwarfs are correlated to  $T_{\text{eff}}$  and mass within the same metal subclass, but it is not the case across different metal subclass. More metal-poor L subdwarfs tend to have higher  $T_{\text{eff}}$ . The  $T_{\text{eff}}$  of L subdwarfs are

<sup>1</sup>Optical and near infrared spectra of new L subdwarfs presented in the series are available online: <https://academic.oup.com/mnras/article-lookup/doi/10.1093/mnras/sty2054#supplementary-data>

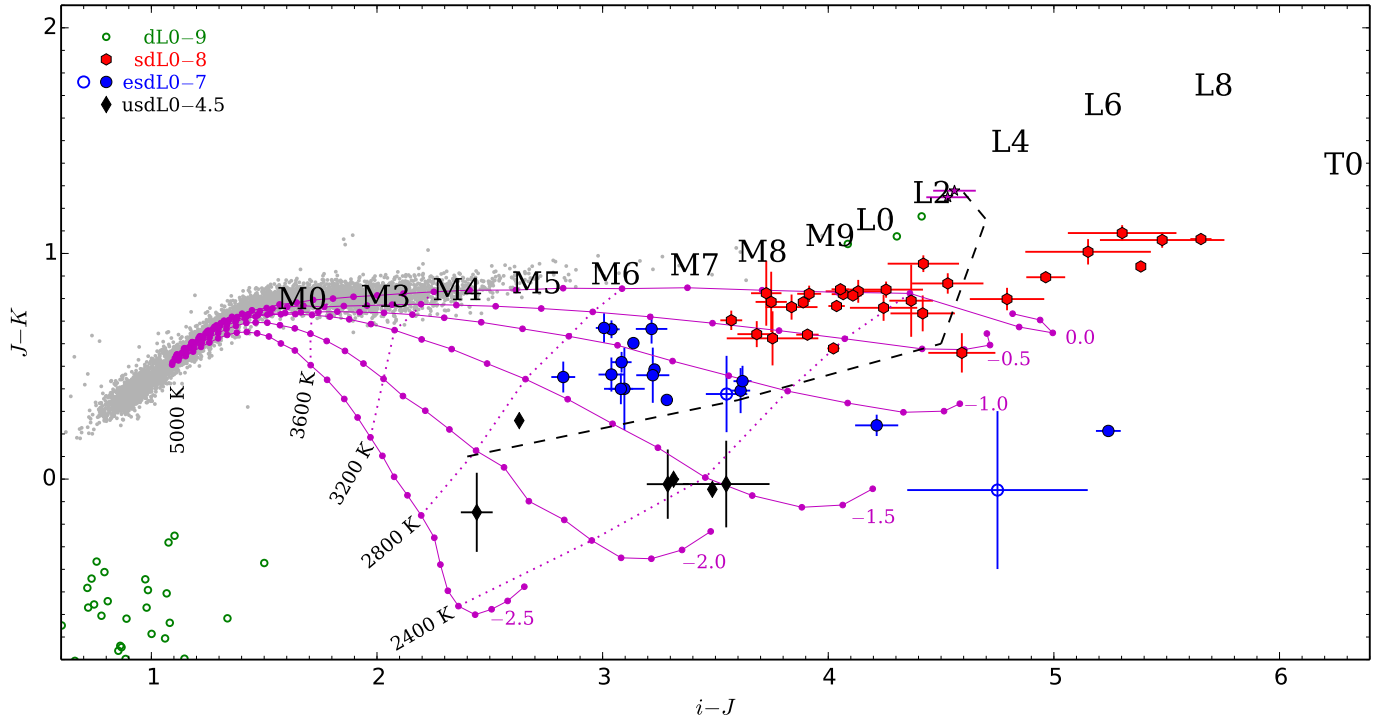


Figure 1: The  $i - J$  vs  $J - K$  colour-colour plot of dL, sdL, esdL and usdL subclasses compared to F, G, K, M, and L dwarfs. A black dashed line indicates the approximate stellar/substellar boundary (fig. 17 of Zhang *et al.*, 2018a).

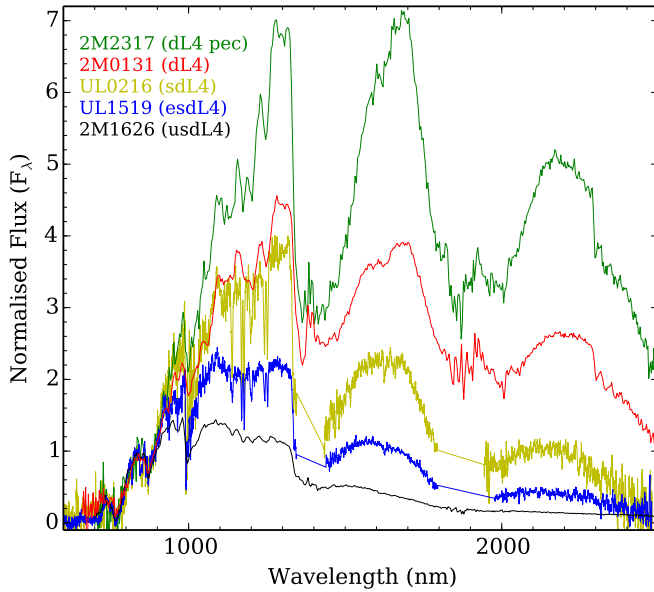


Figure 2: Spectra of red dL4, dL4, sdL4, esdL4, and usdL4 subclasses (modified from fig. 9 of Zhang *et al.*, 2017b). Spectrum of 2MASS J23174712-4838501 (2M2317) is from Kirkpatrick *et al.* (2010), 2MASS J01311838+3801554 (2M0131) is from Burgasser *et al.* (2010), ULAS J021642.96+004005.7 (UL0216) and ULAS J151913.03-000030.0 are from Zhang *et al.* (2017b), 2MASS J16262034+3925190 (2M1626) is from Burgasser (2004).

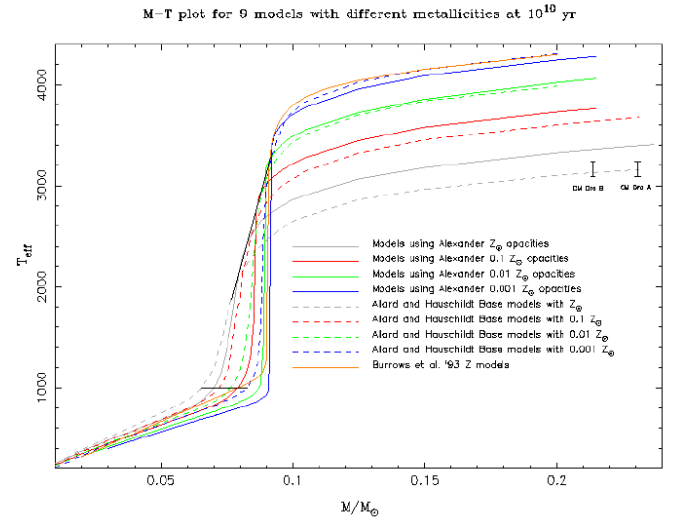


Figure 3: The mass- $T_{\text{eff}}$  isochrones at 10 Gyr for low-mass objects with different metallicity (modified from fig. 5 of Burrows *et al.*, 2001). The black line on top left indicates the HBMM or the stellar boundary on these dashed lines (based on models of Allard & Hauschildt, 1995). A brown dwarf transition zone is below the HBMM and is likely ended at around  $T_{\text{eff}} = 1000$  K, marked with a black line. The mass width of the transition zone is around  $0.012 M_{\odot}$  at  $1-0.01 Z_{\odot}$  and around  $0.0085 M_{\odot}$  at  $0.001 Z_{\odot}$ .

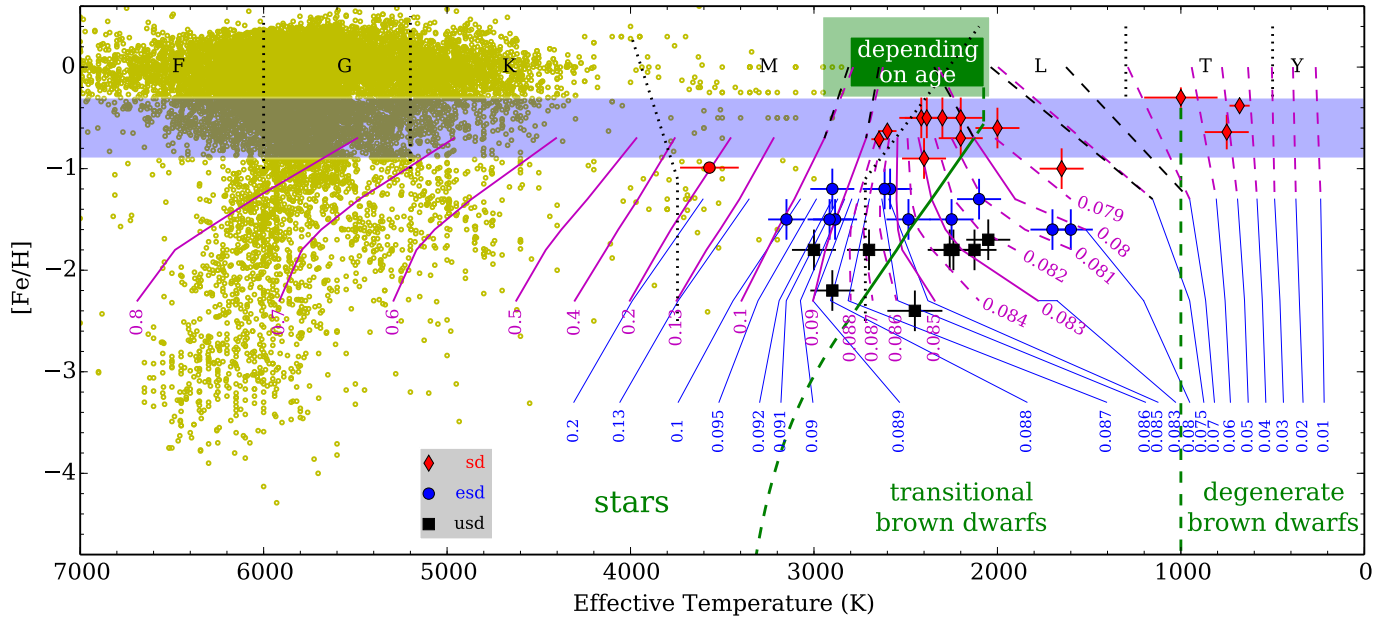


Figure 4:  $T_{\text{eff}}$  versus  $[\text{Fe}/\text{H}]$  of dwarf populations (modified from fig. 9 in Zhang *et al.*, 2017a). The magenta (Baraffe *et al.*, 1997), black (Baraffe *et al.*, 2015), and blue (Burrows *et al.*, 1998) solid/dashed lines indicate iso-mass contours at 10 Gyr. Objects of different spectral classes are divided by black dotted lines. Stars, transitional and degenerate brown dwarfs are divided by solid and dashed green lines. A brown dwarf transition-zone is revealed by the 10-Gyr iso-mass counter (magenta and blue lines; labelled in  $M_{\odot}$ ) between the stellar-substellar boundary and  $T_{\text{eff}} \approx 1000$  K (two green lines; equations 1 and 2 of Zhang *et al.*, 2017a). Yellow circles represent the locus of main sequence stars. This programme is targeting L subdwarfs around this stellar-substellar boundary and in the brown dwarf transition-zone.

higher than similar-typed L dwarfs by around 100–400 K depending on different subclasses and subtypes (e.g. fig. 4 of Zhang *et al.*, 2018b). An L4 type object with lower metallicity is more massive than L4 type objects with higher metallicities. For example, 2M1626 is a halo T-BD with a mass of  $\sim 0.828 M_{\odot}$  (Zhang *et al.*, 2018b). Meanwhile, a young early L type dwarf of an open cluster could fall into the planetary mass domain.

The usdL and esdL subclasses as well as a small fraction of sdL subclass are kinematically associated with the Galactic halo. The sdL subclass are mostly associated with the thick disk.

### 3 Transitional brown dwarfs

The 10-Gyr isochrones of low-mass objects with different metallicity (Fig. 3) show that the  $T_{\text{eff}}$  (and luminosity; figs 4 and 5 of Burrows *et al.*, 2001) of VLMS increases with decreasing metallicity. However, it is reversed below a certain mass where isochrones with different metallicity intersect. The intersection mass is slightly higher at lower metallicity. A steep decline of  $T_{\text{eff}}$ /luminosity as a function of mass is followed after the intersection point. This is because objects with mass below the intersection mass can not maintain steady hydrogen fusion for constant energy supply.

A 10-Gyr isochrone of a certain metallicity intersects with the 10-Gyr isochrone of the metallicity just above/below its own at the mass just below/above the steady hydrogen burning minimum mass (SHBMM) of this certain metallicity. This defines the stellar/substellar boundary of different metallicity. The SHBMM is around 0.08, 0.083, 0.845, 0.855, and 0.875

$M_{\odot}$  at  $[\text{Fe}/\text{H}] = -0.07, -1.3, -1.6, -1.8$ , and  $-2.3$ , respectively (Zhang *et al.*, 2017a), according to evolutionary models (Baraffe *et al.*, 1997; Chabrier & Baraffe, 1997).

The steep decline of  $T_{\text{eff}}$  as a function of mass on the 10-Gyr isochrones in Fig. 3 stop at around 1000 K where the mass is around 0.066–0.083  $M_{\odot}$  (for dashed line with base models of Allard & Hauschildt, 1995) corresponding to 1–0.001  $Z_{\odot}$ , respectively. At below 1000 K,  $T_{\text{eff}}$  decreases slowly with decreasing mass. D-BDs are not massive enough to fuse hydrogen and rely on their initial thermal energy, would cool into the  $\leq 1000$  K domain at 10 Gyr. Note that the  $T_{\text{eff}}$  of D-BDs also decreases with decreasing metallicity, because the lower opacity at lower metallicity leads to a faster dissipation of thermal energy.

The ‘waterfall-like’ feature in Fig. 3 represents a narrow mass range between VLMS and D-BDs, where objects can not maintain their  $T_{\text{eff}}$ /luminosity like stars and also do not cool as fast as D-BDs. Objects in this region are T-BDs (Zhang *et al.*, 2018b). T-BDs are fully convective and could reach temporary states of temperature and pressure sporadically for hydrogen fusion in their cores. The unsteady hydrogen fusion slowly becomes the dominate energy sources to maintain their luminosity. Since the core temperature of a T-BD declines slowly over time. The efficiency of the fusion also declines very slowly over time. The efficiency of the fusion is very sensitive to the mass of T-BDs. Therefore, field T-BDs at a certain age could span in a wide  $T_{\text{eff}}$  range within a narrow mass range. Note the  $T_{\text{eff}}$  range of T-BDs is wider at older age or lower metallicity (Zhang *et al.*, 2018a).

#### 4 The substellar transition zone

The  $T_{\text{eff}}$  distribution of T-BDs is being stretched over time and forming a ‘waterfall-like’ feature at around  $0.07\text{--}0.09 M_{\odot}$  (depending on metallicity; e.g. Fig. 3). The stretching is most significant among halo T-BDs which have  $\sim 10$  Gyr of evolutionary time. Zhang *et al.* (2017a) plotted 10-Gyr iso-mass counters in a  $T_{\text{eff}}$  versus  $[\text{Fe}/\text{H}]$  space (Fig. 4). We can see that for stars with the same mass, those have lower metallicity are also hotter. However, these iso-mass counters between those green lines are stretched towards the low temperature direction, and revealed a ‘substellar transition zone’ - corresponding to the waterfall-like feature revealed by isochrones in Fig. 3.

Halo T-BDs could be separated from VLMS by their  $T_{\text{eff}}$  and  $[\text{Fe}/\text{H}]$ , as they have similar age around 10 Gyr. Halo T-BDs are in a narrow mass range, but they fall into a very broad  $T_{\text{eff}}$  range. Halo T-BDs have  $T_{\text{eff}}$  between 2200–3000 and 1000 K, and spectral types of  $\sim \text{L3--T4}$ . The  $T_{\text{eff}}$  of the stellar/substellar boundary is different across different metallicity (see the left green line in Fig. 4). SDSS J010448.46+153501.8 has the earliest spectral type (usdL1.5) among known halo T-BDs, it is also the most metal-poor substellar object know to date ( $[\text{Fe}/\text{H}] = -2.4$ ).

Although halo T-BDs cover a wide range of spectral types, their number density in the Galaxy is extremely low, because of their narrow mass range on the initial mass function. For example, the transition zone at  $[\text{Fe}/\text{H}] = -1.7$  is around  $0.075\text{--}0.085 M_{\odot}$  and covers a  $T_{\text{eff}}$  range of 2500–1000 K. Currently, there are nine known T-BDs discovered in the Galactic halo with spectral types from usdL1.5 to esdL7 (Zhang *et al.*, 2018b). D-BDs are the majority of BDs, and most of those in the halo have evolved into T5+ and Y subdwarfs.

We draw an empirical stellar boundary on  $i - J$  versus  $J - K$  colour-colour plot (black dashed line in Fig. 1) according to observed colours of L subdwarfs separated by our stellar/substellar boundary in Fig. 4. Fig. 1 also shows that metal-poor substellar objects could be separated by optical and NIR colours sensitive to temperature and metallicity.

Fig. 5 shows solar metallicity isochrones for VLMS and BDs between 0.01 and 10 Gyr. We can see that objects with mass above  $\sim 0.8 M_{\odot}$  could maintain their  $T_{\text{eff}}$  over 10 Gyr. Objects in the grey band are stretched into a wide  $T_{\text{eff}}$  range. Meanwhile, objects with mass below  $\sim 0.7 M_{\odot}$  cool continuously. The different evolution of these objects were governed by their different energy supply channels. VLMS are above the SHBMM, therefore have constant energy supply from hydrogen fusion. T-BDs have unsteady hydrogen fusion to partially replenish the dissipation of initial thermal energy. The efficiency and duration of the fusion is highly depending on their masses. D-BDs have no hydrogen fusion to replenish the dissipation of initial thermal energy.

The existence of the substellar transition zone have impacts on observations and characterization of field BDs. It is difficult to distinguish field T-BDs by spectroscopy and atmospheric parameters, as their luminosity are dominated by their initial thermal energy and have mass/age degeneracy. L type field T-BD are mixed with L type D-BDs that are crossing the substellar transition zone. L type D-BDs with mass less than  $\sim 0.05 M_{\odot}$  could be identified by the 670.8-nm lithium absorption line in their spectra. However, we can not distinguish a T-BD between  $0.06\text{--}0.07 M_{\odot}$  from a D-BD between  $0.06\text{--}0.08 M_{\odot}$  based on their spectra and atmospheric

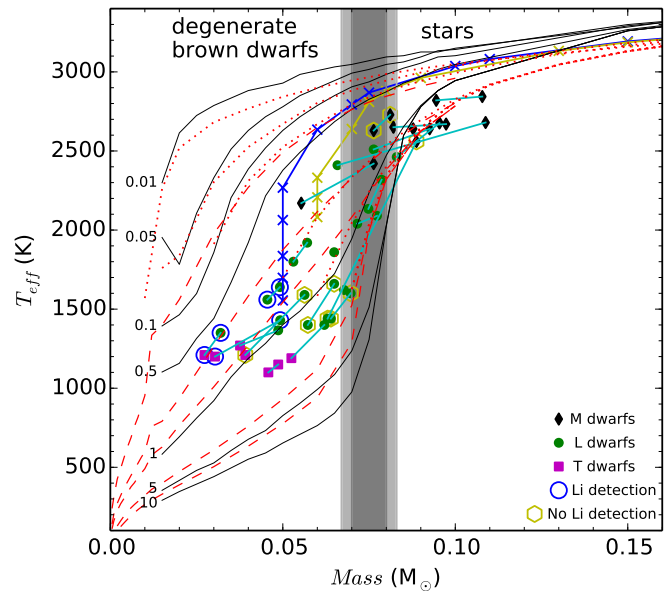


Figure 5: Solar metallicity isochrones for VLMS and BDs at 0.01, 0.05, 0.1, 0.5, 1, 5, and 10 Gyr (modified from fig. 20 of Zhang *et al.*, 2018a). The black, red dashed and dotted lines are isochrones from Burrows *et al.* (1997) and Baraffe *et al.* (2003, 2015), respectively. A grey shaded band indicates the BD transition-zone at solar metallicity, which has a small shift between different model predictions. M, L, and T dwarf companions in binary systems with dynamical mass measurements (Dupuy & Liu, 2017; Lazorenko & Sahlmann, 2018) are also over plotted. Blue and yellow crosses (joined with lines) mark where  $<50\%$  and  $>90\%$  of lithium is depleted, respectively (Baraffe *et al.*, 2015).

parameters.

There is a lack of objects at the L/T transition (Burgasser, 2007). This is firstly because the rapid evolution of BD atmospheres at  $\sim 1200$  K stretched the spectral subtype sampling. Secondly, the L/T transition is at the bottom of the substellar transition zone and next to the abundant D-BDs that crossed the transition zone (Zhang *et al.*, 2018a).

L type D-BDs are younger than cooler T type D-BDs on average according to the isochrones in Fig. 5. However, if we compare the age of a field L dwarf sample and a field T dwarf sample. They should not show much difference. This because a large fraction of field L dwarf sample are T-BDs which are as old as field T dwarfs.

#### 5 Conclusions

T-BDs are a population that different from both VLMS and D-BDs. They have unsteady hydrogen fusion to partially replenish the dissipation of their initial thermal energy, which led to a different evolution and impacted on their observational properties. The substellar transition zone is a stretched temperature canyon of T-BDs in a narrow mass range due to unsteady hydrogen fusion. The substellar transition zone range from 2200–3000 K to 1000 K (depending on metallicity) and from  $\sim \text{L3}$  to T4 types. The moderate evolution of T-BDs and the existence of the substellar transition zone need to be considered in the characterization of BD population.

## Acknowledgments

ZengHua Zhang is supported by the PSL Fellowship.

## References

- Allard, F. 2014, In *Exploring the Formation and Evolution of Planetary Systems*, edited by M. Booth, B. C. Matthews, & J. R. Graham, *IAU Symposium*, vol. 299, pp. 271–272.
- Allard, F. & Hauschildt, P. H. 1995, *ApJ*, 445, 433.
- Baraffe, I., Chabrier, G., Allard, F., & Hauschildt, P. H. 1997, *A&A*, 327, 1054.
- Baraffe, I., Chabrier, G., Barman, T. S., Allard, F., & Hauschildt, P. H. 2003, *A&A*, 402, 701.
- Baraffe, I., Homeier, D., Allard, F., & Chabrier, G. 2015, *A&A*, 577, A42.
- Burgasser, A. J. 2004, *ApJL*, 614, L73.
- Burgasser, A. J. 2007, *ApJ*, 659, 655.
- Burgasser, A. J., Cruz, K. L., Cushing, M., Gelino, C. R., Looper, D. L., *et al.* 2010, *ApJ*, 710, 1142.
- Burgasser, A. J., Cruz, K. L., & Kirkpatrick, J. D. 2007, *ApJ*, 657, 494.
- Burrows, A., Hubbard, W. B., Lunine, J. I., & Liebert, J. 2001, *Reviews of Modern Physics*, 73, 719.
- Burrows, A., Marley, M., Hubbard, W. B., Lunine, J. I., Guillot, T., *et al.* 1997, *ApJ*, 491, 856.
- Burrows, A., Sudarsky, D., Sharp, C., Marley, M. S., Hubbard, W. B., *et al.* 1998, In *Brown Dwarfs and Extrasolar Planets*, edited by R. Rebolo, E. L. Martin, & M. R. Zapatero Osorio, *Astronomical Society of the Pacific Conference Series*, vol. 134, p. 354.
- Chabrier, G. & Baraffe, I. 1997, *A&A*, 327, 1039.
- Dupuy, T. J. & Liu, M. C. 2017, *ApJS*, 231, 15.
- Hayashi, C. & Nakano, T. 1963, *Progress of Theoretical Physics*, 30, 460.
- Kirkpatrick, J. D. 2005, *ARA&A*, 43, 195.
- Kirkpatrick, J. D., Looper, D. L., Burgasser, A. J., Schurr, S. D., Cutri, R. M., *et al.* 2010, *ApJS*, 190, 100.
- Kumar, S. S. 1963, *ApJ*, 137, 1121.
- Lazorenko, P. F. & Sahlmann, J. 2018, *ArXiv e-prints*.
- Nakajima, T., Oppenheimer, B. R., Kulkarni, S. R., Golimowski, D. A., Matthews, K., *et al.* 1995, *Nature*, 378, 463.
- Rebolo, R., Zapatero Osorio, M. R., & Martín, E. L. 1995, *Nature*, 377, 129.
- Zhang, Z. H., Gálvez-Ortiz, M. C., Pinfield, D. J., Burgasser, A. J., Lodieu, N., *et al.* 2018a, *MNRAS*.
- Zhang, Z. H., Homeier, D., Pinfield, D. J., Lodieu, N., Jones, H. R. A., *et al.* 2017a, *MNRAS*, 468, 261.
- Zhang, Z. H., Pinfield, D. J., Gálvez-Ortiz, M. C., Burningham, B., Lodieu, N., *et al.* 2017b, *MNRAS*, 464, 3040.
- Zhang, Z. H., Pinfield, D. J., Gálvez-Ortiz, M. C., Homeier, D., Burgasser, A. J., *et al.* 2018b, *MNRAS*, 479, 1383.